Mapping of hailstorm and strong wind damaged crop areas using LAI estimated from multispectral imagery

J. Furlanetto[1], N. Dal Ferro[1], F. Briffaut[1], L. Carotta[1], R. Polese[1], A. Dramis[2], C. Miele[3], A. Persichetti[3], L. Nicoli[4], F. Morari[1]
[1]*University of Padova, DAFNAE, Legnaro, 35020, Padova, Italy,*
[2]*Società Cattolica di Assicurazione S.C., Verona, 37126, Italy,*
[3]*Archetipo srl, Padova, 35129, Italy,*
[4]*Freelance field inspector, Rovigo, 45100, Italy*
jacopo.furlanetto@phd.unipd.it

Abstract

Hailstorms and strong winds represent a threat to crops, causing defoliation, lodging and in turn yield losses. Crop damages are nowadays assessed by field inspectors, which implies time demanding assessment and difficulties in deriving estimates over large areas. Hailstones and strong wind damage plants through stem breaking, defoliation and lodging, thus leaf area index (LAI) can be a viable tool to detect and quantify the damage level. Here, hailstorm and strong wind damage was artificially caused in a maize field and compared with NDVI-derived LAI from proximal and remote sensing techniques. Estimated LAI was obtained by a NDVI-derived fractional vegetation cover and calibrated light extinction coefficient. Results showed that estimated LAI from remote sensing was able to identify crop damage, with a clear differentiation between leaf damage levels immediately after the event. Following surveys showed a strong recovering capability of maize leading LAI values of damaged treatments to align to those of the control after about 20 days. Remote sensing techniques, coupled with ground measurements, can become a reference tool to assess site-specific hailstorm and strong wind damage over large areas.

Keywords: NDVI, LAI, hail, defoliation, remote sensing.

Introduction

In recent years, extreme weather events such as hailstorms and strong winds are showing an increase in their intensity in Europe, possibly related to temperature changes caused by climate change (Hov et al., 2013). In Central Europe, and particularly in Northern Italy (Po Valley), thunderstorms associated with hailstorms and strong winds are a common phenomenon (Punge et al., 2014), posing a threat to cultivated crops. In maize, hailstones and lodging cause leaf damage as well as plant stem breaking (Vescovo et al., 2016), thus damaging reproductive organs and physiology and in turn affecting yields (Shekoofa et al., 2012). Traditional techniques of hailstorm damage estimation are nowadays questioned, since damage across large fields is hardly quantified. Its estimation by field inspectors is complex and sometimes subjective. Particular attention has been put forth to damage predictions through leaf area index (LAI) and the chlorophyll content (CC) assessments. Their site-specific estimates from remote sensing data might help overcome biased measures from local surveys. The NDVI has been proved effective to detect hail damage (Zhao et al., 2012). In fact, hailstone-related crop defoliation decreases LAI and CC and makes leaf necrosis and large parts of soil visible from sensors (Ali et al., 2015;

Zhao et al., 2012). However, NDVI detection efficacy was questioned by Zhou et al. (2016), who pointed out that plant recovery capabilities could mask the damage signs and symptoms after a certain period of time after the hailstorm event. This study aimed to assess a) whether NDVI from remote sensing could predict maize LAI and detect different levels of hailstorm and strong wind damages, and b) the maize recovery capability in early developing stages and its masking effects.

Materials and methods

Experimental design and treatments

The study was conducted on maize in 2020 at Ca' Tron farm in the Veneto region (Quarto d'Altino, NE Italy, 45°33'21.2"N 12°25'50.6"E). In a 13 ha field, hailstorm and strong wind damage was compared on 18 squared plots of 60×60 m, with two replicates (Figure 1). Hailstorm damage (expected leaf inefficiency –LI– of 20%, 50%, 80%, i.e., leaf area damaged per leaf) and lodging were caused at two plant growing stages, that is 7th leaf (8 plots) and dough stages (8 plots), respectively V7 and R4 stages in the BBCH scale (Bleiholder et al., 2001). Two control plots were included in the experimentation where no damage was caused. The field was managed uniformly throughout the experiment. Maize was sown on May 14th after conventional ploughing and harrowing and fertilized with 280 kg ha^{-1} of mineral 18-46 NP on March 16th and 230 kg N ha^{-1} of urea on May 26th.

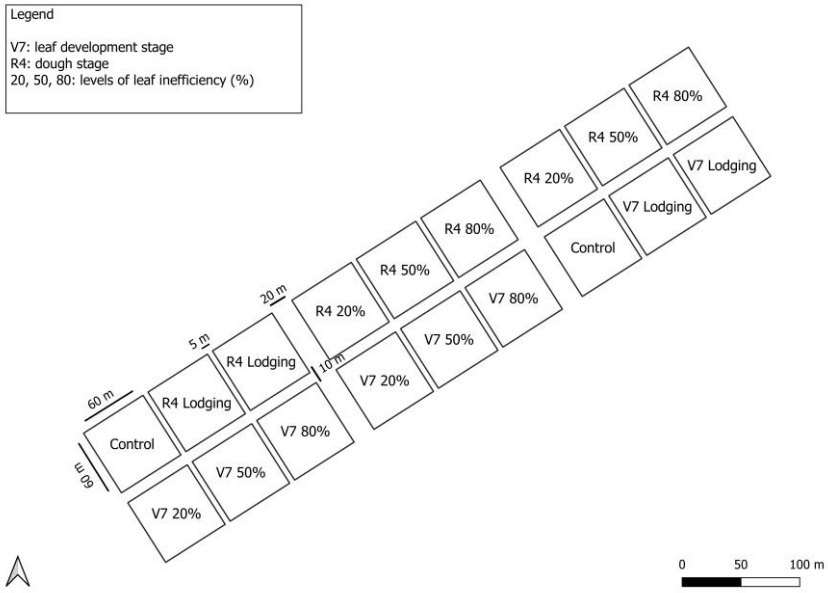

Figure 1. Experimental site location and design. Legend reports treatments.

Simulation of hailstorm damage was caused using two prototype machines, according to maize height. The two prototypes, built at the University of Padova, conceptually work as rotating poles with metal wires attached, which are designed to shred maize leaves at increasing speed. The speed of the rotating poles was adjusted to reach the desired leaf inefficiencies with the support of an insurance field inspector. Conversely, wind damage was caused using a tractor with a front bar adjusted to lodge plants while passing. Damage was caused on June 17th for V7 and on September 9th, 10th and 11th for R4 plant stages. In this study, only damage done at the V7 stage is reported.

Ground monitoring

Ground based measurements were performed on June 19th, July 14th, August 6th and September 16th. Ground surveys were performed on three sampling points per plot, consisting of leaf area index (Accupar LP-80 ceptometer, Meter Group, Pullman, WA, USA), leaf chlorophyll content (Dualex leaf-clip sensor, Force-A, Orsay, France), plant height, fresh and dry biomass and hyperspectral reflectivity. Plant height and biomass were measured on a 1 m^2 area of standing plants while hyperspectral reflectivity was collected with a Fieldspec4 spectroradiometer (Malvern Panalytical, Malvern, UK). The sensing probe allowed approximately for a 0.002 m^2 round area of view.

Remote sensing monitoring

Remote sensing measurements were acquired from both drone-borne sensors and satellite imagery, matching the same dates as the ground monitoring. A preliminary topographic survey was conducted using an RGB Zenmuse X3 camera (DJI, Shenzhen, China) mounted on a Matrice 200 drone (DJI, Shenzhen, China). Known topographic points were detected and used as a reference for NDVI image ortho-rectification, conducted using Metashape software (Agisoft, St. Petersburg, Russia). Multispectral measurements were taken using a Parrot Sequoia sensor (Parrot, USA), mounted on a Matrice 100 drone (DJI, Shenzhen, China). The sensor has a resolution of 1280×960 pixels, working on four spectral regions: green (530-570 nm), red (640-680 nm), far red (730-740 nm) and near infrared (770-810 nm). A 43 flight lines scheme was adopted for all dates, with a side overlay of 85%, a flying height of 55 m and a flight speed of 2.6 m s^{-1}. Sentinel-2 data were used for NDVI calculations as well, including acquisitions available in between the field monitoring dates. NIR (band 8, 785-900 nm) and red (band 4, 650-680 nm) bands have been downloaded and processed.

Data processing and analysis

Proximal and remote sensed NDVI was calculated as follow:

$$NDVI = \frac{NIR - VIS}{NIR + VIS} \quad (1)$$

where NIR and VIS stand for the spectral reflectance measurements acquired in the near-infrared and red (visible) regions, respectively.

After that, remote sensing NDVI imagery was also used to estimate LAI according to Ali et al. (2015):

$$LAI_{NDVI} = \frac{-\log(1 - FVC_{NDVI})}{k(\theta)} \quad (2)$$

where $k(\theta)$ is the extinction light coefficient for a given solar zenith angle, depending also on crop canopy structure, and FVC_{NDVI} is the fractional vegetation cover:

$$FVC_{NDVI} = \frac{NDVI - NDVI_s}{NDVI_v - NDVI_s} \quad (3)$$

where $NDVI_s$ and $NDVI_v$ refer to bare soil (here -0.05) and fully vegetated NDVI (here 0.97) respectively, obtained from NDVI image analysis. In the extreme case in which NDVI would get close to, or equal to, $NDVI_v$, LAI would get close to or reach infinite.

Thus, obtained LAI values were capped to 7. A homogenous $k(\theta)$, equal to 0.37, was calibrated using ground measured LAI and estimated FVC in Eq. (2) by aggregating measured data from all monitoring dates and minimizing the RMSE between measured ($LAI_{measured}$) and simulated ($LAI_{simulated}$) LAI.

Results

Simulated leaf inefficiency (LI) reflected real hailstorm effects by ripping and shredding leaves. Its magnitude, as assessed by field inspectors, was lower than the expected one especially at medium and high intensity (actual LI=20%, 35%, 51%), maintaining though the treatments differentiation. Ground-based surveys (Table 1) after V7 damage showed a slight reduction in the chlorophyll content on June 19th between LI80% (40.2 µg cm^{-2}) and the other treatments (43.5 µg cm^{-2}). Similar results were also detected for dry biomass (1.9 Mg ha^{-1} vs 2.5 Mg ha^{-1} on average). Proximal sensed NDVI, calculated on single leaves and not over canopy, did not show significant differences between treatments. Values were influenced only by plant growth stage and therefore proximal NDVI was not reported nor used for deriving LAI. NDVI from remote sensing varied according to damage. On June 19th (2 days after damage), both drone and satellite highlighted a NDVI gradient mirroring the LI gradient. On this date, drone camera (5x5 cm ground resolution) showed an average value of 0.45 in LI20%, 0.36 in LI50% and 0.27 in LI80% compared to 0.49 in control treatment and 0.48 in lodging (standard errors in table 1). Differences in NDVI became negligible in the following dates (14th July, 6th August) with both sensors. Satellite NDVI values (ground resolution of 10x10 m) were higher than drone ones, +15% on average, showing the greatest difference on June 19th (+28%). Both ground-measured and simulated LAI (Figure 2) reflected a gradient that was clearly visible just after damage (19th June). Higher LAI values were found in the control (1.41 measured and 2.37 average simulated from drone and satellite) compared to damaged plots (1.31, 1.21, 0.82 measured; 1.96, 1.64, 1.26 average simulated from drone and satellite, respectively on LI20%, 50%, 80%). Estimated LAI, both drone and satellite, was on average higher than measured LAI. Nonetheless, a good regression was found between measured and both drone-estimated (R^2=0.94, RMSE=0.54) and satellite-estimated (R^2=0.95, RMSE=1.39) LAI. Treatments did not show significant differences between measured LAI, while they did for drone-estimated ($p<0.01$) and satellite-estimated ($p<0.01$) LAI. Ground-measured LAI showed less damage gradient than estimated LAI. On June 17th, prior to damage –image was acquired a few hours before damage– estimated LAI from satellite (Figure 2C) had similar LAI levels in all treatments. On June 19th, after the damage, a differentiation was visible both from drone and satellite (Figure 2B-C): LAI slightly increased in the control while decreased in the other plots according to the damage level. This differentiation was clearly visible until July 7th. Afterward, no clear differences were detectable among treatments. Notably, lodged treatment did not show an overall estimated LAI reduction just after the damage, but did only later with lower values compared to hail and control treatments. The spatial visualization of drone-borne derived LAI is reported in Figure 3. On 19th June, damaged plots were visibly distinguishable from control plot, lodged plots and those only later subjected to damage in R4 stage. On the following dates, the pattern of recovery previously highlighted is clearly visible, showing a slight reduction in crop yield, being 8.89 Mg ha^{-1} in the control compared to an average yield loss of -1.58 Mg ha^{-1} with damage.

Table 1. Average±standard error values for ground measured chlorophyll content, dry biomass and NDVI from drone-borne camera and satellite after V7 simulated damage.

	Chlorophyll (µg cm^{-2})				Dry biomass (Mg ha^{-1})			
	19th Jun	14th Jul	6th Aug	16th Sep	19th Jun	14th Jul	6th Aug	16th Sep
LI 20%	42.5±2.1	44.6±1.9	41.4±2.2	38.1±1.7	2.6±0.2	16.6±0.4	15.4±0.6	19.3±1.3
LI 50%	44.0±2.1	43.3±1.3	45.4±1.0	41.7±1.3	2.1±0.1	15.8±0.3	15.1±1.1	18.2±0.9
LI 80%	40.2±2.2	43.1±1.4	43.6±1.9	39.6±2.0	1.9±0.1	15.6±0.4	13.9±0.4	18.6±0.7
Lodging	44.1±1.3	43.7±1.0	42.5±2.7	37.0±2.8	2.4±0.2	19.5±1.0	16.2±0.5	17.3±0.8
Control	43.5±1.9	42.6±1.0	43.8±2.3	38.3±2.9	1.9±0.1	16.0±0.2	14.4±0.6	16.6±1.3
	NDVI (drone)				NDVI (satellite)			
	19th Jun	14th Jul	6th Aug	16th Sep	19th Jun	14th Jul	6th Aug	16th Sep
LI 20%	0.45±0.02	0.81±0.01	0.81±0.00	-	0.58±0.02	0.88±0.00	0.89±0.00	0.53±0.03
LI 50%	0.36±0.01	0.80±0.01	0.80±0.00	-	0.50±0.01	0.88±0.00	0.89±0.00	0.57±0.02
LI 80%	0.27±0.02	0.79±0.01	0.79±0.00	-	0.41±0.02	0.86±0.01	0.88±0.00	0.56±0.02
Lodging	0.48±0.02	0.81±0.00	0.77±0.00	-	0.60±0.01	0.85±0.00	0.86±0.00	0.45±0.02
Control	0.49±0.02	0.83±0.01	0.80±0.01	-	0.62±0.01	0.88±0.01	0.89±0.00	0.53±0.03

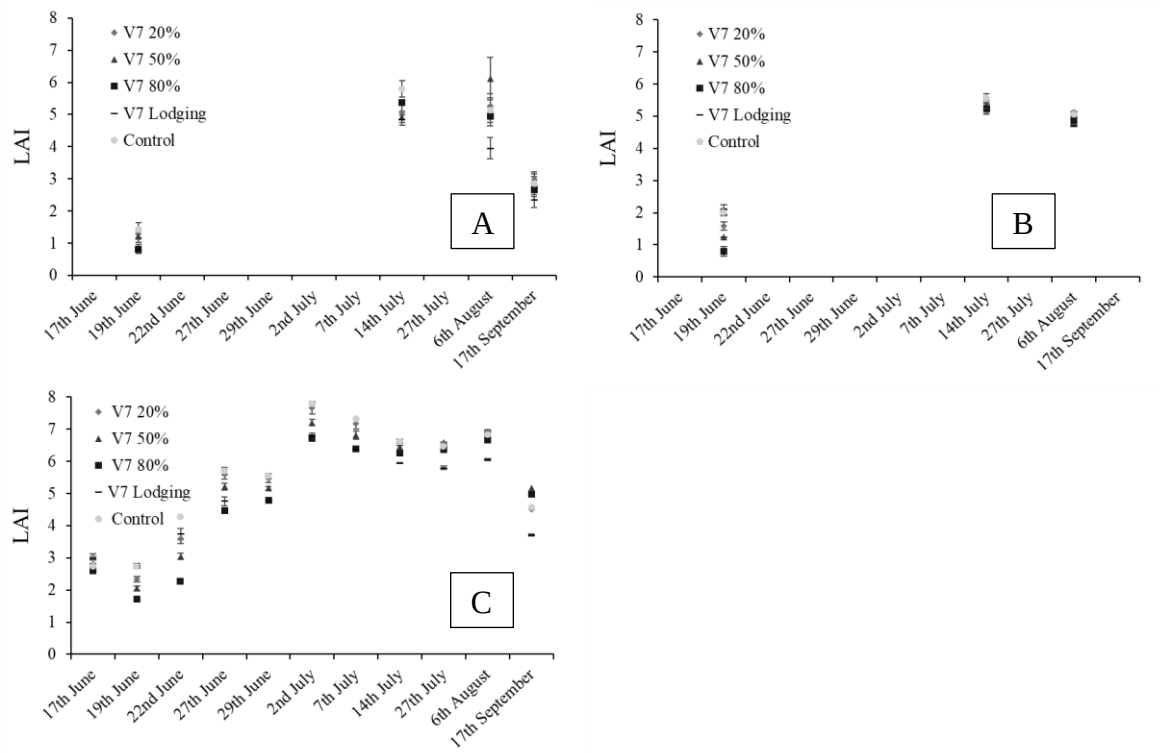

Figure 2. (A) ground measured LAI average values; (B) drone-borne simulated LAI average values; (C) Sentinel-2 simulated LAI average values after V7 simulated damage

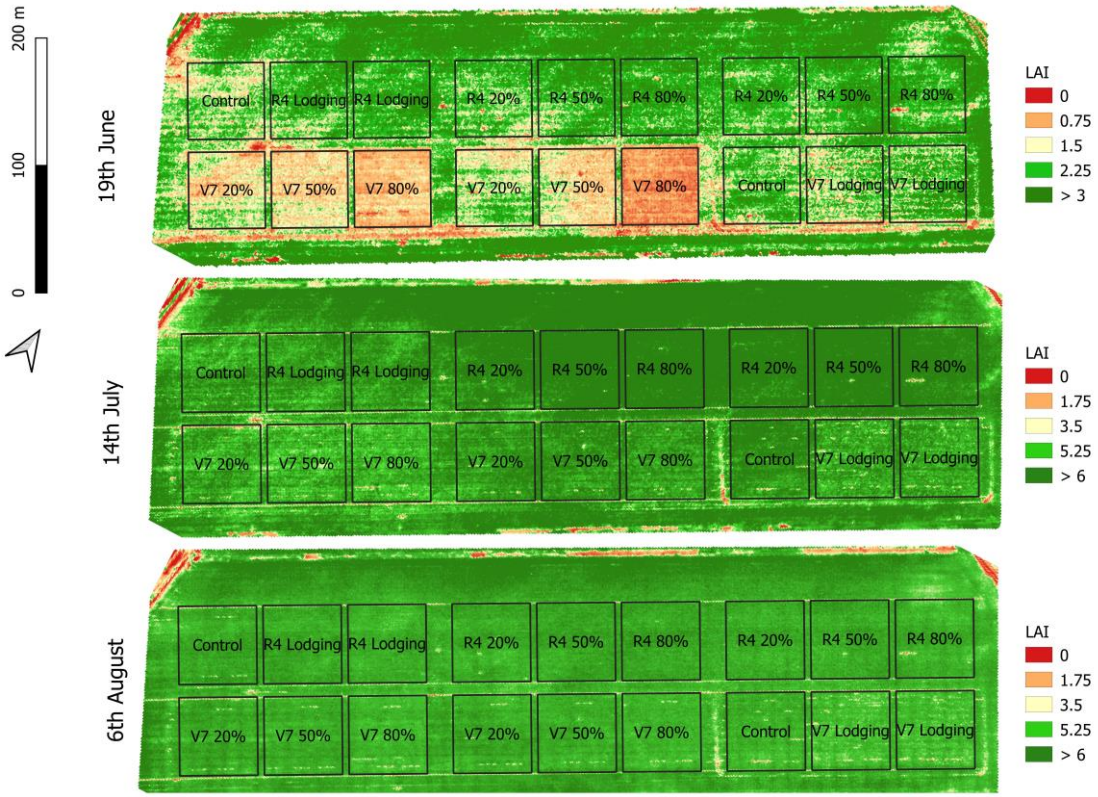

Figure 3. Drone-borne NDVI-derived LAI images from the surveys conducted on June 19th, July 14th and August 6th, 2020, after V7 simulated hailstorm damage. 20%, 50% and 80% represent the leaf inefficiency levels.

Discussion

Chlorophyll content did not show a strong gradient within damage treatments and compared to control. It was hypothesized that proximal sensing did not catch the leaf inefficiency because surveys were conducted close to the simulated damage. Moreover, on the successive dates, new leaves had grown and damaged leaves aged. Chlorophyll damage evolution was therefore not detected. Similarly, NDVI retrieved from field sensor did not show differences between damaged and undamaged plots, likely due to the sensor intrinsic operation. A 0.002 m^2 circular area was visible to the instrument probe, which was almost entirely occupied by plant green organs that did not represent the full crop canopy. As also suggest by Raper et al., (2013), differences in NDVI are seen between near leaf and full canopy measurements, with proximal sensors saturating earlier than wider field of view sensors (full canopy). As a result, any leaf necrosis was observed using proximal sensing, which in turn suggests the importance of NDVI measures done over the whole canopy and not only at the leaf scale for detecting hail damage. In contrast, remote sensing surveys revealed differences between damaged and undamaged plots just after the simulated hailstorm event. The maize fractional vegetation cover (FVC) was reduced by leaf breaking and removal, following the damage gradient, and the maize canopy structure was modified. NDVI from remote sensors appeared to be more sensitive to these changes, likely due to the influence of more bare soil visible to the sensor after damage. This would explain the better performance in damage detection of wide-area viewing sensors such as satellites or drone-borne ones when compared to proximal (leaf and stem level) NDVI

retrieval techniques. In this study, a homogeneous light extinction coefficient $k(\theta)$ was used for estimating LAI. While $k(\theta)$ is likely to change mainly due to canopy structure over maize cropping season, a single average value was here used, obtained by averaging single $k(\theta)$ calculated for each monitoring date. This allowed to obtain standardized LAI estimates throughout the season, similarly to Brogi et al., (2020) and in line with average values by Flénet et al., (1996). Thus, using equation 2 allowed to calibrate a single $k(\theta)$ crop-specific value and evaluate whether its application would lead to reliable LAI estimates. A coherent differentiation between damage is visible on June 19th both in measured and estimated LAI. Notably, ground measured LAI showed a differentiation in the post damage surveys (July 14th, August 6th) which appeared to be weakly related to damage, thus highlighting the point-dependent sampling measurements. Estimated LAI (Figure 3) detected a spatial variability within plots, thus possibly explaining the difficulties of ground measured LAI to account for consistent differences between treatments. In both drone and satellite estimated LAI, the distinction between damage levels progressively decreased moving forth from the date of the damage. Notably, LI80% showed a slower recovery capability compared to LI20% and LI50%, in accordance with the higher defoliation level. Nonetheless, maize at all damage levels showed a recovery behavior, which was caused by the development of new leaves (damage was done at the 7th leaf stage) which gradually covered the damaged ones, therefore preventing remote sensing detection. This behavior would also explain the lack of LAI differences in drone imaging on July 14th and following survey. Wide-area simulated LAI will prove helpful for obtaining input values for crop simulation models, overcoming limited sampling point capability over large fields.

Conclusions

It was observed that NDVI retrieved from multispectral remote sensors can be an effective index for deriving wide-area LAI estimates using a NDVI-LAI calibrated model. The model is based solely on the light extinction coefficient and measured NDVI. This might help in detecting hail damaged areas quickly and on large portions of land, integrating and sustaining field monitoring by insurance inspectors. The estimated LAI was related to different hail damage levels in maize. A gradient of LAI index response was highlighted when compared to damage levels. This is due to the increasing defoliation following different levels of damage, that can be detected by the NDVI index used for calculation. Use of a proximal NDVI sensor did not prove effective for the purpose of this study, since it was not able to detect the full canopy effects of wide-area defoliation or leaf necrosis just after damage nor in the following dates due to emission of new leaves. Use of remote sensors proved effective in detecting and differentiating damage, highlighting though an important issue of this method, that is the time span. LAI values appeared to follow a plant recovery period (14-20 days) after which damage was not anymore detectable. Further research at different plant stages is needed to assess temporal dynamics of LAI recovery, thus detecting the specific time span in which LAI index can be efficiently used to identify and eventually quantify the damage.

References

Ali, M., Montzka, C., Stadler, A., Menz, G., Thonfeld, F., Vereecken, H. (2015). Estimation and validation of RapidEye-based time-series of Leaf Area Index for winter wheat in the Rur catchment (Germany). *Remote Sensing*, *7*(3), 2808–2831. https://doi.org/10.3390/rs70302808

Bleiholder, H., Eichhorn, K., Klose, R., Lorenz, D., Meier, U., & Weber, E. (2001). Growth stages of mono and dicotyledonous plants BBCH Monograph. *Federal Biological Research Centre for Agriculture and Forestry*.

Brogi, C., Huisman, J. A., Herbst, M., Weihermüller, L., Klosterhalfen, A., Montzka, C., et al. (2020). Simulation of spatial variability in crop leaf area index and yield using agroecosystem modeling and geophysics-based quantitative soil information. *Vadose Zone Journal*, *19*(1), 1–24. https://doi.org/10.1002/vzj2.20009

Flénet, F., Kiniry, J. R., Board, J. E., Westgate, M. E., Reicosky, D. C. (1996). Row spacing effects on light extinction coefficients of corn, sorghum, soybean, and sunflower. *Agronomy Journal*, *88*(2), 185–190. https://doi.org/10.2134/agronj1996.00021962008800020011x

Hov, Ø., Cubasch, U., Fischer, E., Höppe, P., Iversen, T., Kvamstø, N. G., et al. (2013). Extreme Weather Events in Europe: preparing for climate change adaptation, *Norwegian Meteorological Institute, (Issue October).*

Punge, H. J., Bedka, K. M., Kunz, M., Werner, A. (2014). A new physically based stochastic event catalog for hail in Europe. *Natural Hazards*, *73*(3), 1625–1645. https://doi.org/10.1007/s11069-014-1161-0

Raper, T. B., Varco, J. J., & Hubbard, K. J. (2013). Canopy-based normalized difference vegetation index sensors for monitoring cotton nitrogen status. *Agronomy Journal*, *105*(5), 1345–1354. https://doi.org/10.2134/agronj2013.0080

Shekoofa, A., Emam, Y., Pessarakli, M. (2012). Effect of partial defoliation after silking stage on yield components of three grain maize hybrids under semi-arid conditions. *Archives of Agronomy and Soil Science*, *58*(7), 777–788. https://doi.org/10.1080/03650340.2010.546788

Vescovo, L., Gianelle, D., Dalponte, M., Miglietta, F., Carotenuto, F., Torresan, C. (2016). Hail defoliation assessment in corn (Zea mays L.) using airborne LiDAR. *Field Crops Research*, *196*, 426–437. https://doi.org/10.1016/j.fcr.2016.07.024

Zhao, J. L., Zhang, D. Y., Luo, J. H., Huang, S. L., Dong, Y. Y., Huang, W. J. (2012). Detection and mapping of hail damage to corn using domestic remotely sensed data in China. *Australian Journal of Crop Science*, *6*(1), 101–108.

Zhou, J., Pavek, M. J., Shelton, S. C., Holden, Z. J., Sankaran, S. (2016). Aerial multispectral imaging for crop hail damage assessment in potato. *Computers and Electronics in Agriculture*, *127*, 406–412. https://doi.org/10.1016/j.compag.2016.06.019